

Article

Effect of Fe(II)-Activated Peroxymonosulfate (PMS) on the Performance of Ultrafiltration (UF) Process for Secondary Effluent Treatment and Reuse

Xiao Liu, Renglu Chen, Zijing Wang, Wei Lin, Rourou Zhang, Shengping Yu and An Ding * 

State Key Laboratory of Urban Water Resource and Environment (SKLUWRE), School of Environment, Harbin Institute of Technology, 73 Huanghe Road, Nangang District, Harbin 150090, China; lx08050623@163.com (X.L.); crl15815200587@163.com (R.C.); 3825835042@163.com (Z.W.); hitlinweiwwl@163.com (W.L.); zhangrrhit@163.com (R.Z.); yushengping2022@163.com (S.Y.)

* Correspondence: dinganhit@163.com

Abstract: The secondary effluent of the wastewater treatment plant is considered as one of the reused water sources and needs advanced treatment to meet increasingly stringent water treatment standards. Ultrafiltration, as one of the most widely used advanced treatment technologies, is limited due to membrane fouling, and coagulation and pre-oxidation have received extensive attention as pretreatment methods to alleviate membrane fouling. This research proposes a new method of Fe(II)-activated peroxydisulfate (PMS) coagulation and a pre-oxidation system coupled with ultrafiltration (UF) to treat secondary effluent from sewage plants, separately evaluating the treatment effect under different molar ratios of Fe(II)/PMS. The Fe(II)/PMS decontamination mechanism and membrane fouling control effect were elucidated through pollutant removal efficiency, membrane morphology, membrane flux trend, and membrane fouling resistance distribution. According to the experimental results, the optimal effect of organic matter removal and membrane fouling mitigation was achieved at the Fe(II)/PMS dosage of 60/60 $\mu\text{M}/\mu\text{M}$ (molar ratio 1:1). The efficiency of pretreatment methods in removing organics and fluorescent components and mitigating membrane fouling followed the order of Fe(II)/PMS > Fe(III) > inactivated PMS. Fe(II)/PMS could produce a synergistic effect in a high concentration state (60 μM), relying on the dual effects of coagulation and oxidation to alleviate membrane fouling. Coagulation and pre-oxidation by Fe(II)/PMS significantly reduced the clogging of membrane pores and the proportion of irreversible resistance, effectively controlling membrane fouling and improving effluent quality. SEM images further confirmed its effectiveness, and EPR results unequivocally indicated that its synergistic mechanism was mediated by $\bullet\text{OH}$ and $\text{SO}_4^{\bullet-}$. The research results can provide ideas for advanced wastewater treatment and secondary effluent reuse.

Keywords: ultrafiltration; membrane fouling; coagulation; pre-oxidation; ferrous-activated peroxydisulfate; secondary effluent



Citation: Liu, X.; Chen, R.; Wang, Z.; Lin, W.; Zhang, R.; Yu, S.; Ding, A. Effect of Fe(II)-Activated Peroxymonosulfate (PMS) on the Performance of Ultrafiltration (UF) Process for Secondary Effluent Treatment and Reuse. *Water* **2022**, *14*, 1726. <https://doi.org/10.3390/w14111726>

Academic Editor: Jesus Gonzalez-Lopez

Received: 26 April 2022

Accepted: 25 May 2022

Published: 27 May 2022

Publisher's Note: MDPI stays neutral with regard to jurisdictional claims in published maps and institutional affiliations.



Copyright: © 2022 by the authors. Licensee MDPI, Basel, Switzerland. This article is an open access article distributed under the terms and conditions of the Creative Commons Attribution (CC BY) license (<https://creativecommons.org/licenses/by/4.0/>).

1. Introduction

Water is the basic condition for human existence and an irreplaceable resource that supports the social and economic system [1]. Resource recovery is a virtuous circle, not just providing more sustainable resources but also reducing costs for water utilities [2]. Under the background of today's era, sewage treatment has become an important part of the urban water resource cycle. By the end of 2017, China's daily sewage treatment capacity was about 193 million tons, accounting for about 20% of the global sewage treatment scale [3]. The discharge of pollutants from industry, cities, and agriculture has increased, and the progressively serious water pollution problem has put forward higher requirements for urban sewage treatment facilities [4]. The stable secondary effluent after biological sewage treatment is a reliable water source for reuse. However, the effluent after secondary

treatment still contains a considerable amount of pollutants, bacteria, etc., and needs to be equipped with advanced treatment processes such as disinfection or membrane technology to improve water quality, reducing negative impacts on public health [5,6].

Membrane filtration has been recognized as an effective advanced treatment method with a small footprint, superior performance in removing organic matter and retaining microorganisms, and can produce higher quality and safer water, making it a competitive option of increasing interest [3]. As a typical process of membrane technology, ultrafiltration (UF), with a membrane pore diameter of 5–100 nm, can effectively remove bacteria, colloids, suspended solids, and even harmful substances in water [7]. However, in wastewater treatment plants, UF has insufficient ability to remove small molecular organics and membrane fouling. Membrane fouling, as the main obstacle to low-pressure membrane technology, will lead to increased operation and maintenance costs, and needs to be assisted by means of physical backwashing, disinfection, and chemical cleaning [8,9]. The main contributors for membrane fouling are protein-rich biopolymer fouling layers, humic acids, colloids, etc. [10,11]. Although the permeability of the membrane can be partially restored by physical backwashing, owing to the serious irreversible fouling of UF processing, frequent physical cleaning will shorten the life of the membrane [7]. Chemical cleaning also cannot fully restore the original performance and permeability of the membrane, resulting in a decrease in membrane filtration performance over time [12]. Therefore, many studies have turned their attention to pretreatment of membranes. For membrane fouling, current widely used pretreatment methods include coagulation, pre-oxidation, adsorption, etc., but a single method cannot completely remove the targeted foulants, and there are still some small molecular organic substances and bacteria that may accumulate on the membrane or block membrane pores [13]. Combination processes have been extensively studied, among which various coagulation–oxidation synergistic processes such as Fe(II)-KMnO₄, Fe(II)-PMS, Al (III)-O₃, etc., which have achieved relatively excellent fouling mitigation effects [14–16].

FeSO₄ is a common low-cost coagulant with high activity and environmental friendliness, and PMS has more general activation properties than persulfate (PS) and H₂O₂, owing to its lower energy of the lower unoccupied molecular orbital [17–19]. The feasibility and high efficiency of the co-processing of the two have been demonstrated, due to the bidirectional action of coagulation and oxidation, and they have been applied in the pretreatment of membrane technology for surface water, micro-pollutants such as carbamazepine (CBZ) and sulfamethoxazole (SMX), and sludge dewatering [15,20,21]. In previous studies, Cheng et al. evaluated the effect of using Fe(II)/PMS as a membrane pretreatment method to treat natural organic matter in a ceramic membrane UF system under neutral conditions, and later evaluated the removal efficiency of natural organic matter and sulfate anions in the nanofiltration (NF) system [19,22]. There may be some differences between the secondary effluent of the sewage plant, the natural water, and the water quality simulated by the experiment, so it is necessary to evaluate the treatment effect of this pretreatment method in real water.

In this study, the recommendations of optimal molar ratio were provided for the removal of TOC in the secondary effluent. On this basis, with Fe(II)/PMS as the core, the removal of organic matter, fluorescent components, and nitrogen and phosphorus nutrients in effluent was studied by analogy to Fe(III) coagulation and un-activated PMS pre-oxidation. The effect and mechanism of the three methods in the mitigation of membrane fouling were studied. The membrane fouling was characterized by a scanning electron microscope (SEM), the oxidation mechanism was explored by electron paramagnetic resonance (EPR), and a fouling fitting model was constructed. This research is of great value to the application of wastewater reuse, and the research results can also provide new insight into advanced wastewater treatment and secondary effluent reuse.

2. Materials and Methods

2.1. Preparation of Feed Water

To simulate the real situation, the secondary effluent used in this study was directly taken from the Harbin Xinyi Wastewater Treatment Plant. The secondary treatment process adopted by this plant was the Anaerobic-Anoxic-Oxic (AAO) process. The water samples were taken from the front end of the ultraviolet (UV) disinfection process. The experimental water temperature was maintained at 19–21 °C. The specific raw water quality parameters were shown in Table S1.

2.2. Experimental Setup

2.2.1. Pretreatment with Fe(II)-PMS

In this study, Fe(III) coagulation, un-activated PMS, and Fe(II)-activated PMS were adopted as pretreatment strategies for the UF process. Ferric chloride (FeCl_3) used as a coagulant was purchased from Tianjin Xinbote Chemical Co., Ltd. Tianjin, China. Potassium hydrogen peroxymonosulfate $\text{KHSO}_5 \cdot \text{KHSO}_4 \cdot \text{K}_2\text{SO}_4$ used as an oxidant was obtained from Shanghai Aladdin Biochemical Technology Co., Ltd. Of China, and ferrous sulfate (FeSO_4) used as an activator was obtained from Tianjin Jizhun Chemical Technology Co., Ltd. Tianjin, China. All research reagents were commercially available and adopted without purification. Ultrapure water was used in the solution preparation and backwashing process involved in the experiment.

The polyvinylidene fluoride (PVDF) UF membranes used in this study were purchased from Microdyn Nadir Company of Germany (Wiesbaden, Germany), whose molecular weight cut-off was 150 kDa. Diaphragm diameter was 76 mm and the membrane area was 45 cm², while the effective filtration area after subtracting the apron was 38 cm². The membrane was soaked in 30% ethanol for 30 min before use, and then washed three times with ultrapure water for subsequent process.

The coagulation experiment was carried out at room temperature (17–21 °C), taking 1 L of raw water, and adding a certain dose of Fe(III) to the water sample to initiate the reaction. Appropriate doses of PMS were added to a certain concentration of Fe(II) samples for pre-oxidation experiments. The coagulant dosage used in the coagulation experiment was 0, 30 and 60 µmol/L. The dosage of Fe(II)/PMS used in the Fe(II)-activated PMS experiment included: 0/0, 0/30, 0/60, 30/30, 60/60, 120/120, 15/60, 30/60, 90/60, 120/60, 60/15, 60/30, 60/90, 60/120 µM/µM. A six-link electric stirrer (MY3000-6G, MeiYu, Hubei, China) was adopted with rapid mixing for 1 min at 200 r/min, followed by slow mixing for 20 min at 50 r/min. After stirring, the water samples were taken and stored at 4 °C, and then immediately put into the UF device for filtration without precipitation.

2.2.2. Membrane Filtration

The device mainly involved in this study was a flat-sheet UF membrane device, mainly composed of a nitrogen cylinder, a pressure reducing valve, an ultrafiltration cup (Amicon 8200, Millipore, Billerica, MA, USA) with a maximum volume of 500 mL, an electronic balance, and a computer connected to an automatic control and information acquisition software. The experiment was performed in filtration cells with constant pressure dead-end mode. The filtration pressure was provided by a nitrogen cylinder, and the transmembrane pressure (TMP) was maintained constant and controlled at about 0.07 MPa for each filtration. Figure 1 shows the experiment setup of UF, Fe(III)-UF, PMS-UF, and Fe(II)/PMS-UF. The operating process of the membrane filtration was as follows.

The pretreated UF membrane was placed face up at the bottom of the ultrafiltration cup. An amount of 300 mL of the water sample to be filtered was taken and put into the ultrafiltration cup, and filtered under pressure. The backwashing water was ultrapure water of 200 mL, and the backwashing pressure was 0.1 MPa. In the experiment of measuring membrane flux, each ultrafiltration membrane was filtered for three cycles. When conducting experiments related to membrane characterization, in order to ensure that the

surface morphology of the membrane was not damaged, only one cycle of filtration was performed, including ultrapure water filtration and water sample filtration.

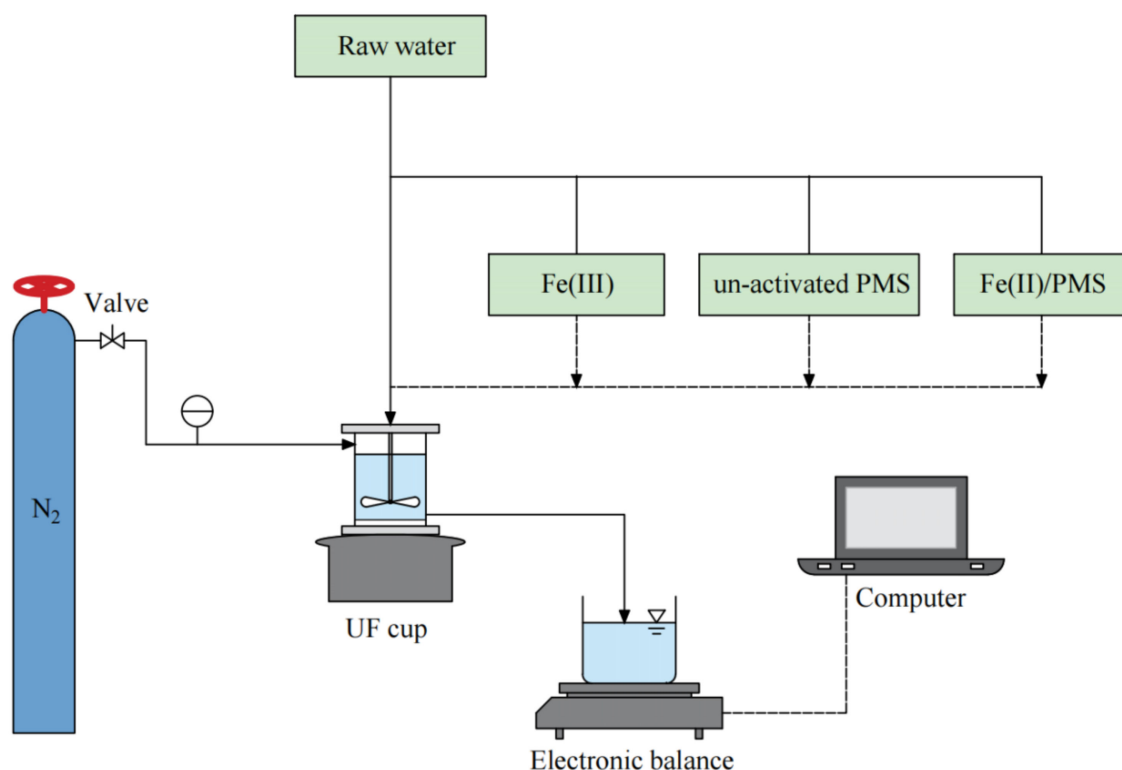


Figure 1. Ultrafiltration system setup.

2.3. Analytical Methods

2.3.1. Characteristics of Effluent and Membrane

In the experiment, the efficiency of the coagulation and pre-oxidation UF system in treating the secondary effluent of the sewage plant was investigated, so it is necessary to measure the quality of the raw water and the effluent after UF, so as to deduce the practicability and feasibility of the system. Total organic carbon (TOC) of water samples was detected by a total organic carbon analyzer (Multi N/C 2100S, Jena, Germany). UV_{254} was tested by a UV/vis spectrophotometer (T6, Xinchiji, Beijing, China) at the wavelength of 254 nm. Polysaccharide and protein were also determined by this apparatus, using the phenol sulfuric acid method [23] and the Lowry method, respectively [24]. Total phosphorus (TP) was measured by ICP-OES (Optima 8300, PerkinElmer, Waltham, MA, USA), total nitrogen (TN) was measured by a TOC analyzer (TOC-VCPN, Shimadzu, Kyoto, Japan), and a pH meter (PB-10, Sartorius, Germany) was used to measure pH value.

In order to further characterize the concentration of organic matter in the water, fluorescence excitation-emission matrix (EEM) was also employed to characterize the fluorescence intensity of water samples. The EEM spectra were generated by a fluorescence spectrophotometer (F7000, Hitachi, Tokyo, Japan) with excitation (Ex) wavelengths of 200–450 nm at an interval of 5 nm and emission (Em) wavelengths of 250–550 nm at an interval of 1 nm. The samples for analysis included the raw water samples obtained after adding the reagents and stirring, the raw water samples prefiltered through 0.45 μm membranes, the effluent after UF process, and the effluent samples filtered through 0.45 μm membranes. To eliminate the influence of Raman scattering, the EEM spectrum of ultrapure water was subtracted before samples analysis.

Electron paramagnetic resonance (EPR) spectroscopy (A200S-95/12, Bruker, Germany) was used to detect free radicals $\bullet\text{OH}$ and $\text{SO}_4^{\bullet-}$ formed in the Fe(II)/PMS system and 5,5-dimethyl-1-pyrroline-N-oxide (DMPO, 97%, MACKLIN) was used as a spin-trapping agent.

Then, 1 mL of standard sample and 50 μL of DMPO were prepared. The spectroscopy settings included a microwave frequency of 9.852 GHz and microwave power of 7.290 mW.

Scanning electron microscope (SEM) (ZEISS Sigma 500, Oberkochen, Germany) was applied to observe the fouling of the UF membrane after secondary effluent filtration and the characterization of the micromorphological changes on the membrane surface after Fe(II)/PMS pretreatment.

All of the above analyses were performed at room temperature of 300 K.

2.3.2. Membrane Resistance Evaluation

In order to further analyze the water purification efficiency of coagulation and coagulation-oxidation treatment, this research also studied the total membrane resistance and resistance distribution of UF membranes. The resistance-in-series model was used to evaluate the fouling resistance [25,26]. The membrane resistance was analytically calculated by Darcy Law Equation (1).

$$J = \frac{TMP}{\mu R_t} \quad (1)$$

$$R_t = R_m + R_f \quad (2)$$

$$R_f = R_r + R_{ir} \quad (3)$$

where J is the permeate flux ($\text{L}/(\text{m}^2 \cdot \text{h})$), TMP is the transmembrane pressure (Pa), μ is the dynamic viscosity ($\text{Pa} \cdot \text{s}$), R_t is the filtration total resistance (m^{-1}). The total resistance (R_t) consists of intrinsic membrane resistance (R_m) and membrane fouling resistance (R_f), while R_f consists of reversible resistance (R_r) and irreversible resistance (R_{ir}). Before filtering the water sample, under the same external conditions, the R_m of the UF membrane was measured by filtering the ultrapure water. After the water sample was filtered for the first time, the ultrapure water was filtered again to obtain the R_t , and the R_f of the UF membrane could be obtained according to Equation (2). After the first backwash, the ultrapure water was filtered again to obtain the sum of the R_m and R_{ir} . Finally, the R_{ir} and R_r could be calculated by Equation (3).

2.3.3. Fouling Model Fitting

Membrane fouling is the main reason hindering the development of membrane filtration. Membrane flux decreases owing to accumulation of contaminants on the membrane surface and in the membrane pores. When the particle diameter is smaller than the pore size, the particles will enter the pores and cause pore blockage, while when the particle diameter is larger than the pore size, the particles will accumulate on the membrane surface to form a fouling layer. Under constant pressure conditions, the flux decrease in dead-end filtration can be explained by different fouling models, including complete blocking, standard blocking, incomplete blocking, and sediment filtration. In the complete blocking model, it is assumed that the voids are completely blocked by particles, not allowing fluid to pass through, and there is no overlap between the particles, meaning the pollution layer is a single layer and the blocking area is proportional to the filtration volume. In the standard blocking model, it is assumed that the particles are deposited on the walls of the membrane pores and the pore volume decreases are proportional to the permeation volume. For the incomplete blocking model, it is assumed to be similar to the complete blocking model, but the particles can overlap, meaning the probability that the particles block the membrane pores is not 100%. The sediment filtration model assumes that particles accumulate on the membrane surface, stacking and assembling to form a filter cake layer [27,28]. The mathematical equations of the four types of fouling models are shown in Table 1.

Table 1. Types and causes of membrane fouling models.

Models	Causes	Flux and Resistance Model
Complete blocking	Pore Blockage	$J_0 - J = AV$
Standard blocking	Direct adsorption	$1/t + B = J_0/V$
Incomplete blocking	Long-term adsorption	$\ln J_0 - \ln J = CV$
Cake filtration	Boundary layer resistance	$1/J - 1/J_0 = DV$

Where, A , B , C , and D are constants, V is the filtration volume, t is the filtration time, and J_0 is the initial permeate flux.

3. Results and Discussion

3.1. Effect of Fe(II)/PMS Molar Ratio on TOC Removal

To evaluate the influence of coupled Fe(II) and PMS with different molar ratios on the optimization of raw water quality, the water quality before UF membrane permeation was determined and the concentration of organic components (TOC) after administration is illustrated in Figure 2. When the PMS concentration remained at 60 μM , and the Fe(II) concentrations were set at 0, 15, 30, 60, 90, and 120 μM , the average TOC concentration decreased from 9.06 to 7.88, 7.42, 6.86, 6.74, and 6.86 mg/L, respectively. TOC gradually decreased with Fe(II) dosage, but decreased indistinctively when the Fe(II) concentration rose to 60 μM . This is owing to the oxidation of Fe(II) into Fe(III) by the presence of PMS. The in situ formed Fe(III) acted as a coagulant, was hydrolyzed, and eventually formed positively charged complexes under neutral conditions, which strongly interacted with negatively charged colloidal substances and then agglomerated into larger particles or flocs, followed by interception and removal in the subsequent membrane process [29–31]. When Fe(II) concentration was fixed at 60 μM , the PMS concentrations varied in the range of 0, 15, 30, 60, 90, and 120 μM , TOC concentration turned out to be 12.09, 10.41, 10.15, 9.00, 8.48, and 8.07 mg/L, respectively. TOC gradually decreased with the PMS dosage. This phenomenon was due to the fact that PMS acted as an oxidant, converting macromolecular organics in the secondary effluent into small molecules or mineralized pieces [15,32]. The experimental results could also indicate that under the same molar dosage of Fe(II) and PMS, the coupling function led to better removal efficiency of organic matter than the individual application. The effect of 90 μM coagulant was slightly superior to that of 60 μM coagulant, but high doses of coagulant may lead to secondary pollution due to excessive residual iron content in the effluent. Iron residue may cause the water to darken and be unacceptable to the public [33]. Therefore, the follow-up evaluation of the coupling effect for the system and the membrane treatment was carried out under the optimal molar ratio of 1:1.

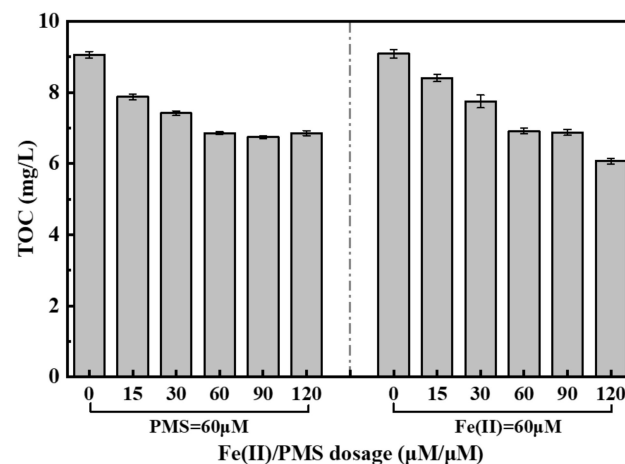


Figure 2. Pollutants in the feed water of UF under different molar ratios of Fe(II)/PMS: concentrations of TOC.

3.2. Application Advantages of Fe(II)/PMS-UF Treatment

3.2.1. Removal of TOC and UV₂₅₄

Using Fe(III) coagulation/PMS oxidation as pretreatment methods, the quality of the effluent after the UF membrane was tested. The raw water was set as the control group, and the remaining second to eighth groups were added in the influent with 30 μM PMS, 30 μM Fe(III), 30 μM Fe(II)/30 μM PMS, 60 μM PMS, 60 μM Fe(III), 60 μM Fe(II)/60 μM PMS, and 120 μM Fe(II)/120 μM PMS. Figure 3a shows the removal efficiency of TOC and UV₂₅₄ under the Fe(II)/PMS molar ratio as 1:1 (concentration gradients of 30/30, 60/60 and 120/120 $\mu\text{M}/\mu\text{M}$). UV₂₅₄ has a strong correlation with the content of aromatic carbon and is usually used to represent aromatic compounds in DOC, usually hydrophobic NOMs such as humic substances [22,34]. Compared with the control group, the TOC removal rates of the second to eighth groups were 4.2%, 13.0%, 14.2%, 6.5%, 21.4%, 29.3%, and 35.8%, respectively. It can be seen that the removal effect of inactivated PMS alone on TOC was limited, and Fe(III) alone had a better effect, while the removal effect of PMS coupled with Fe(II) activation surpassed that of PMS and Fe(III) alone. In this study, when the molar ratio was 1:1, the removal rate of TOC increased with the dosage going up, and compared with the data of Section 3.1, TOC values decreased as a whole, implying that ultrafiltration had a certain retention effect on TOC. Compared with the effluent of the control group, the UV₂₅₄ values of the remaining groups decreased by 3.7%, 12.2%, 23.4%, 6.4%, 31.9%, 46.3%, and 49.5%, respectively, which showed the same trend as the TOC results.

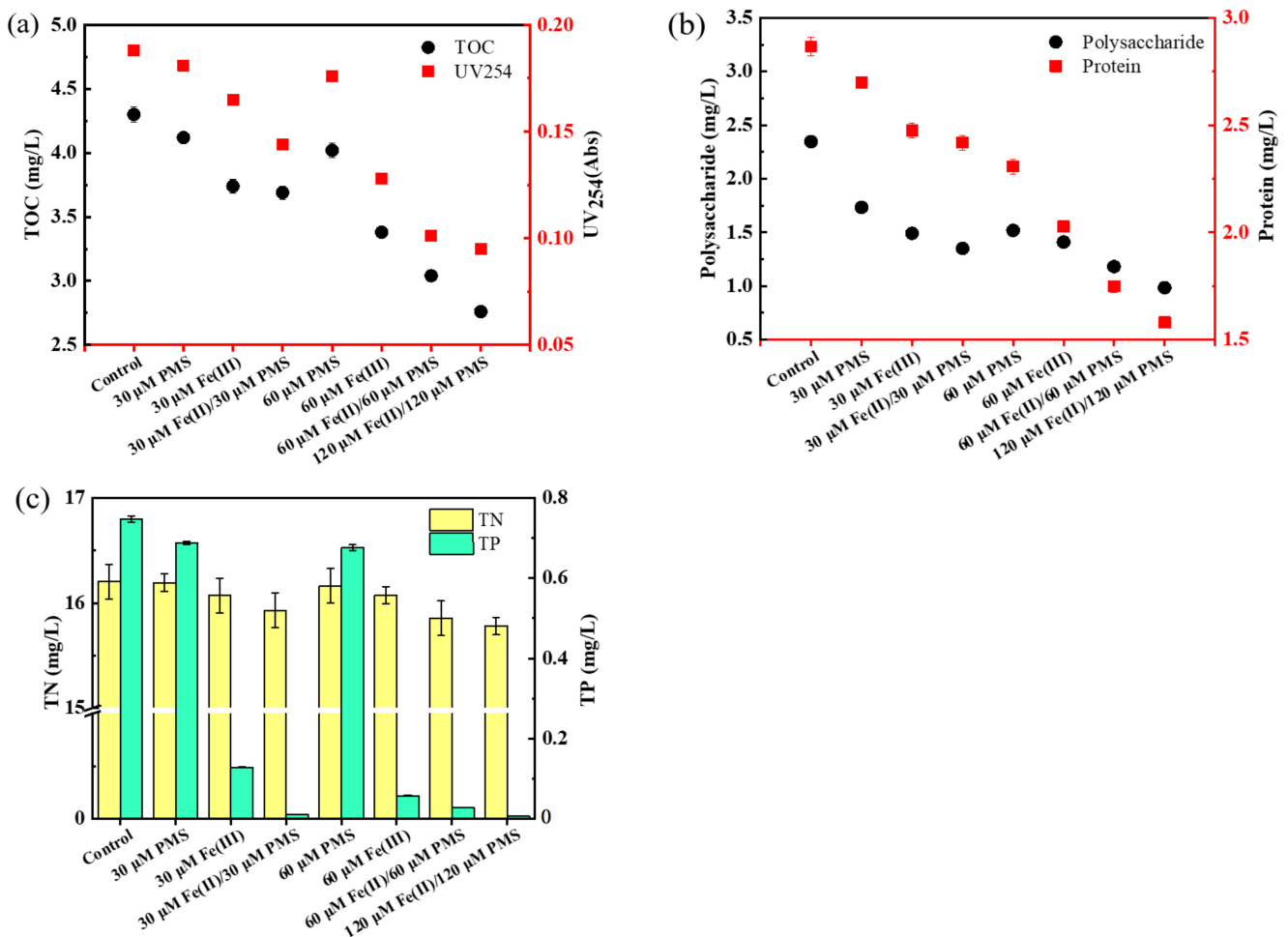


Figure 3. Pollutants in the permeate water of UF under different conditions: (a) concentrations of TOC and UV₂₅₄; (b) concentrations of polysaccharide and protein; (c) concentrations of TN and TP.

The results exhibited that Fe(II)/PMS pretreatment was superior to Fe(III) coagulation and PMS oxidation with the same molar dosage in removing TOC and UV₂₅₄, and the effect was gradually optimized with the increase in the input amount. Organic pollutants cannot always be efficiently oxidized and decomposed by oxidants, and thus activation methods were adopted to promote the oxidation reactions [35]. According to previous studies, PMS is a precursor of sulfate radicals, which can generate sulfate radicals and hydroxyl radicals under conditions such as photolysis, pyrolysis, or chemical activation [35,36]. Meanwhile, Fe(II) was oxidized to Fe(III) by PMS, acting as an activator and forming a coagulant in situ. The Fe(II)/PMS system coupled the dual effects of advanced oxidation and coagulation to significantly degrade organic pollutants in the secondary effluent.

3.2.2. Removal of Macromolecular Organics

In addition to TOC and UV₂₅₄, macromolecular organic proteins and polysaccharides were also determined. As shown in Figure 3b, detecting effluent after pretreatment and ultrafiltration, the protein concentrations of the second to eighth groups reduced by 5.8%, 13.6%, 15.6%, 19.5%, 29.2%, and 39.0%, and polysaccharides reduced by 44.8%, 36.4%, 42.4%, 35.3%, 39.9%, 49.6%, and 58.0%, respectively, compared with the control group. It can also be concluded that the removal efficiency followed the order: Fe(II)/PMS > Fe(III) > inactivated PMS. Both the proteins and polysaccharides contributed to membrane fouling. In the early stage of membrane filtration, hydrophobic proteins deposited on the membrane surface, thereby reducing the permeability of the membrane, and soluble polysaccharides were more likely to cross-link to form a gel layer, which may cause worse membrane fouling than proteins [37,38]. The gel layer was formed by non-covalent bonds in the connecting regions and forms a continuous three-dimensional network, while the interaction of proteins and polysaccharides was also non-covalent [39]. Sulfate radicals generated by Fe(II)-activated PMS broke the non-covalent bonds through oxidation, and degraded macromolecular substances into small molecules, thereby reducing the concentrations of proteins and polysaccharides [40]. This synergistic effect was superior to individual coagulation or oxidation because it combined the dual effects of coagulation and oxidation, while ordinary oxidation was converted into a more effective advanced oxidation.

3.2.3. Removal of Fluorescent Organics

EEM spectra have been used to characterize organic components such as protein and humic acid in river water, domestic sewage, and the secondary effluent during ultrafiltration and nanofiltration [41]. The impact of Fe(II)/PMS on the fluorescent components of secondary effluent from the Harbin Xinyi sewage treatment plant was investigated, the intensity values of fluorescent substances in water before and after UF are shown in Table S2, and the EEM spectra of fluorescent components in effluent after membrane are presented in Figure 4. According to the research by Yu and Graham [14], the EEM spectra was divided into four regions: Region A (Ex/Em = 235–240/340–355 nm, aromatic proteins), Region B (Ex/Em = 275–280/320–330 nm, tryptophan-like components), Region C (Ex/Em = 240–260/390–445 nm, fulvic-acid-like components), and Region D (Ex/Em = 290–350/410–435 nm, humic-acid-like components). For influent before UF, when only inactivated PMS was added regardless of the concentration, tryptophan-like components (Peak B) and fulvic-acid-like components (Peak C) were not significantly weakened, while aromatic proteins (Peak A) and humic-acid-like components (Peak D) slight decreased, and the order followed: inactivated PMS > Fe(III) coagulation > Fe(II)/PMS. However, when only Fe(III) was added, the four main peaks all performed a downward trend. Compared with the results of Fe(II)/PMS dosing, it implied that coagulation in Fe(II)/PMS was responsible for the removal of fluorescent components [15]. This can be attributed to that the complexes formed by the coagulant metal and fluorescent organics in the flocs can quench the fluorophore, influencing fluorescence measurements through light absorption, scattering, and even shading [42,43]. The activated PMS also had a certain removal effect on the fluorescent components in the secondary effluent, and when the

molar ratio was 1:1, the higher the dosage, the better the removal effect. For the effluent after membrane filtration, when only inactivated PMS was added, the four main peaks did not show a clear downward trend, while Fe(III) coagulation contributed to the decline of the four main peaks, also verifying the previous conclusion. At the same time, the intensity of fluorescent components decreased after the UF process, indicating that UF can intercept substances such as protein and humic acid to a certain extent.

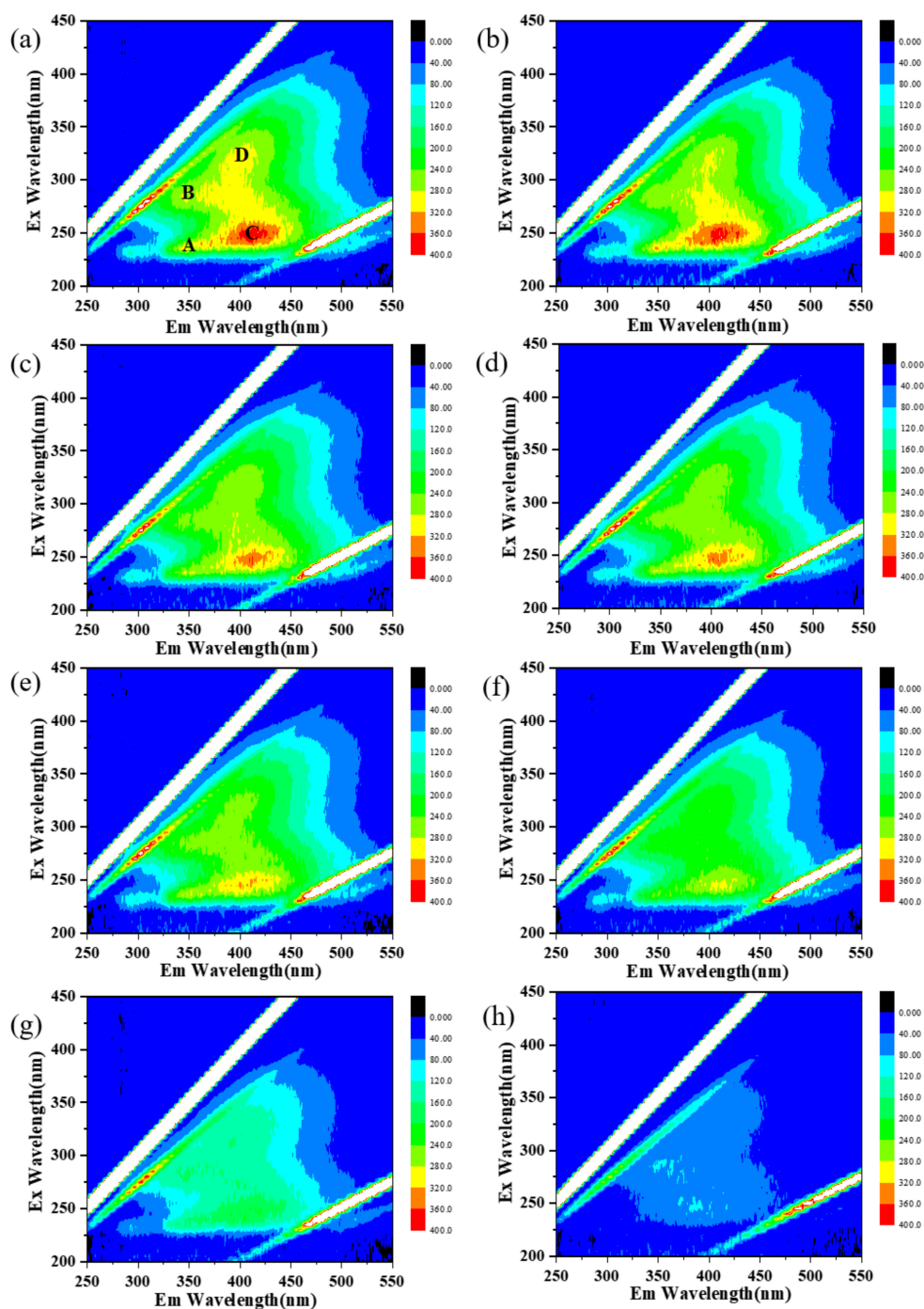


Figure 4. Fluorescence EEM spectra of organic matters in the permeate water of UF under different concentrations of Fe(II)/PMS: (a) control; (b) 30 μM PMS; (c) 60 μM PMS; (d) 30 μM Fe(III); (e) 60 μM Fe(III); (f) 30/30 $\mu\text{M}/\mu\text{M}$ Fe(II)/PMS; (g) 60/60 $\mu\text{M}/\mu\text{M}$ Fe(II)/PMS; and (h) 120/120 $\mu\text{M}/\mu\text{M}$ Fe(II)/PMS.

3.2.4. Removal of TN and TP

Nutrient elements such as nitrogen and phosphorus can cause eutrophication, which will lead to environmental and ecological problems, such as algal blooms and freshwater resource pollution [44]. Therefore, the nitrogen and phosphorus elements in the effluent of the UF membrane after pretreatment were detected. Figure 3c reveals that the TN concentrations leveled off, and that for the eight groups of membranes were 16.20, 16.19, 16.07, 15.93, 16.16, 16.07, 15.86, and 15.78 mg/L, respectively. Compared with the raw water, the TN removal rate of each group was less than 10%, owing to that the added chemicals did not produce obvious biological effects. Fe coagulation and PMS oxidation failed to effectively process removing nitrogen with a minimal effect. Generally speaking, there is basically no nitrogen removal effect for coagulants prepared from Fe or Al. Coagulation combined with complexation or other complex mechanisms may be required for nitrogen removal [45].

However, the concentration of TP was greatly affected by dosing, and especially in groups with 30/30, 60/60, and 120/120 $\mu\text{M}/\mu\text{M}$ Fe(II)/PMS, the removal rate of TP compared with raw water can reach 98.7%, 96.5%, and 99.2%, respectively. It can be seen from the results that the synergistic pretreatment of Fe(II)/PMS had a good removal effect on TP, and coagulation played a major role. As reported by Liu et al. [46], the combination of coagulation and ultrafiltration could remove about 80% of phosphorus. The iron salt was hydrolyzed to form a variety of polymeric cations, which reduced the zeta potential of the particles and promoted instability. The greater amount of iron coagulant dosage triggered the better phosphorus removal efficiency [47]. Phosphorus was removed through a combination of charge neutralization, bridge formation, and scanning solidification mechanisms [48]. As the oxidant in the system, PMS can achieve a phosphorus removal efficiency of about 10%, compared with the control group. The combination of the two can reduce the phosphorus concentration to a trace amount, meeting the TP discharge standard for domestic surface water [49].

3.3. Membrane Fouling Control

3.3.1. Membrane Morphology Characterization

Figure 5 presents the SEM image of the ultrafiltration membrane surface after Fe(II)/PMS pretreatment of the secondary effluent. The SEM images showed clear membrane pores on the surface of the new membrane (Figure 5a), different pore sizes, relatively uniform distribution, and the unpolluted membrane surface without any foulants. After filtering the secondary effluent, the membrane (Figure 5b) surface was evenly covered by foulants, and a portion of the foulants entered the membrane pores, forming a smooth and dense cake layer. At the same time, some pollutants with larger particles on the membrane surface were clearly visible. After pretreatment with different agents, it can be clearly seen that the surface of the membrane presented different morphologies. When treated with 60 μM PMS, the fouled membrane began to expose some membrane pores, and the filter cake layer was damaged to a certain extent. When treated with 60 μM Fe(III), a porous and loose agglomerate cake layer was formed on the membrane surface, which delayed the decrease in membrane flux [50]. The Fe(II)/PMS system, owing to its superior oxidation and coagulation performance, significantly destroyed membrane fouling and formed flocs with larger particles, and the cake layer was more loose and porous. The obvious floc pores provided a larger number of water passages for the water flow, which was beneficial to the recovery of the membrane flux and the subsequent backwashing of the cake layer.

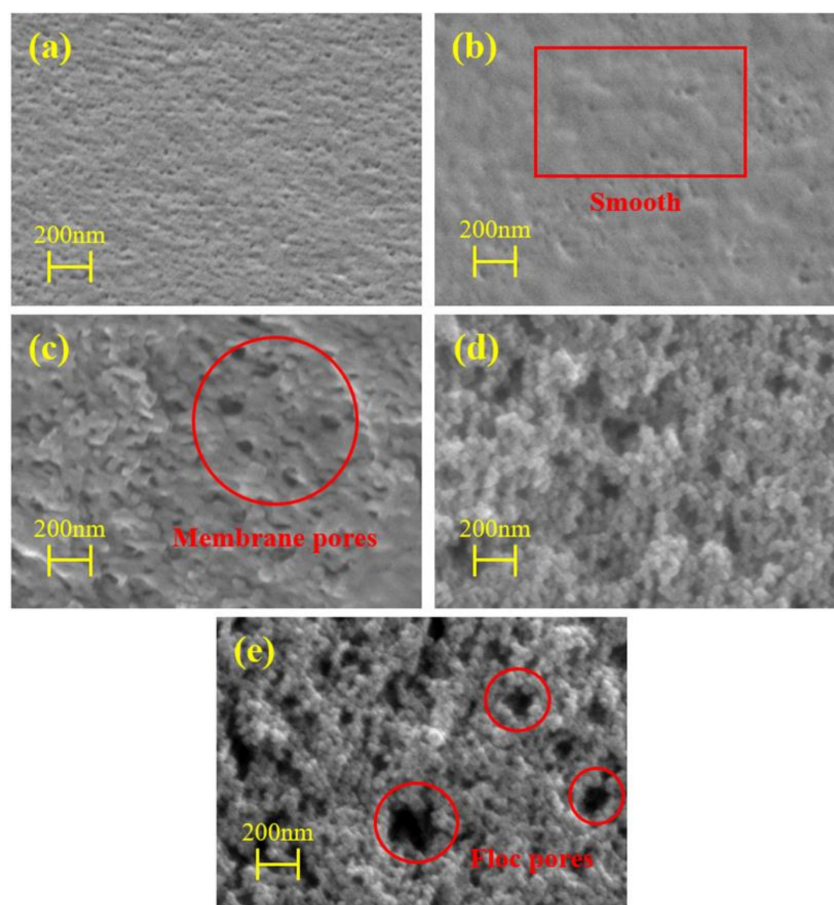


Figure 5. SEM images of membrane surface: (a) original membrane; membrane after (b) raw water filtration; (c) pretreatment of 60 μM PMS; (d) pretreatment of 60 μM Fe(III) and (e) pretreatment of 60 μM Fe(II)/60 μM PMS. Conditions: EHT = 15 kV, Mag = 20.00 KX.

3.3.2. Membrane Flux Development

The flux variations in the UF system with different concentrations of PMS, Fe(III), and Fe(II)/PMS pretreatment are illustrated in Figure 6. The raw water without any pretreatment caused the severe flux decline, and at the end of the three cycles under low (30 $\mu\text{mol/L}$) and high (60 $\mu\text{mol/L}$) concentrations, the specific flux (J/J_0) decreased to about 0.18 LWH. Under the condition of low concentration (30 $\mu\text{mol/L}$), PMS oxidation had limited improvement on the specific flux; at the end of each cycle, the specific flux (J/J_0) was about 0.21 LWH. Fe(III) coagulation significantly enhanced membrane fouling control with a specific flux of 0.25 LWH at the end of each cycle. In the Fe(II)/PMS group, the mean specific flux at the end of three cycles was about 0.27 LWH under the dual effects of coagulation and oxidation. Similarly, under the condition of high concentration (60 $\mu\text{mol/L}$), the flux changes caused by different pretreatment methods showed the same trend. When only PMS was added for oxidation, the J/J_0 at the end of each cycle was about 0.20 LWH, and it was about 0.24 LWH under the condition of Fe(III) coagulation, while in the Fe(II)/PMS group, the specific flux at the end of the three operation cycles was 0.30 LWH under the dual effects of coagulation and oxidation. Compared with raw water, after three cycles of hydraulic backwashing, the flux recovery rate of Fe(II)/PMS at 30 $\mu\text{mol/L}$ and 60 $\mu\text{mol/L}$ could reach 50% and 67%, respectively, so the synergy of them was extremely helpful for flux recovery.

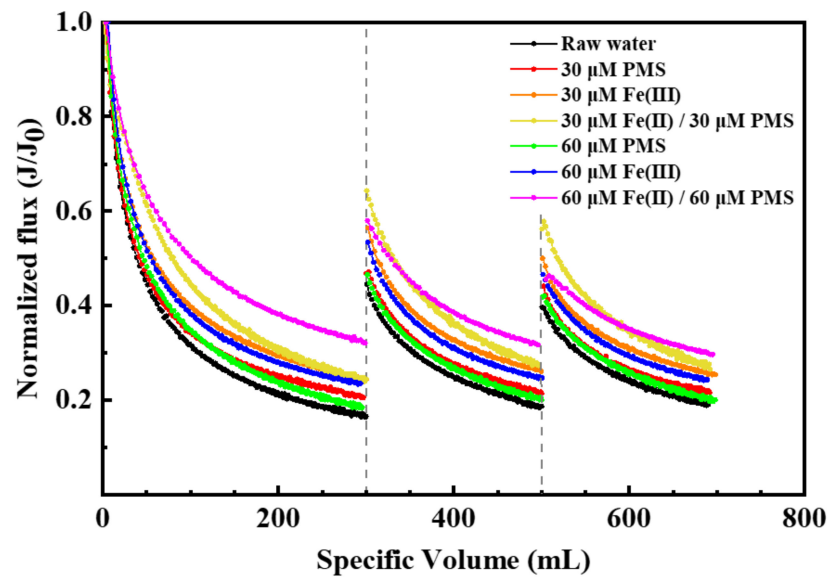


Figure 6. Changes of specific flux (J/J_0) with filtration volume (mL) under different concentration conditions.

It can be seen from the experimental results that PMS oxidation can remove some organics, oxidizing macromolecules into small molecules, while the oxidation ability of inactivated PMS was limited, giving rise to the limited ability to mitigate membrane fouling. Fe(III) coagulation alleviated membrane fouling by removing organics through binding with insoluble flocs, and the ability was slightly stronger than that of oxidation, while both oxidation and coagulation were taken into account by Fe(II)/PMS, leading to optimum membrane fouling mitigation. Cheng et al. [22] found that at the same iron dosage, the Fe(II)/PMS combination was better than Fe(III) coagulation alone in restoring membrane flux. Fan et al. [51] also found that the membrane flux of the Fe(II)/PMS-UF group increased by 65%, 84%, and 99% in three filtration cycles, respectively, which was due to the dual effects of coagulation and oxidation, and they were convinced that the mechanisms of coagulation and oxidation on membrane flux promotion were different. Coagulation removes pollutants by generating flocs to adsorb insoluble pollutants, forming micro-flocs to visible suspended particles, which will gradually precipitate during the subsequent stationary period, forming a sludge mass as shown in Figure 5 [52]. The larger sludge produced may cause clogging of the UF membrane pores, which may be the reason for the lower specific flux at the end of the cycle with 60 μM Fe(III) than with 30 μM Fe(III). The PMS molecule is asymmetrical ($^-\text{O}_3\text{SO}-\text{OH}$), with the attached sulfite (SO_3^-) on one side and hydrogen on the other side, which is more susceptible to nucleophilic attack by electron-rich organics, thereby oxidizing certain electron-rich organic pollutants through electron transfer [53,54]. However, due to its weak oxidative capacity, its fouling mitigation is far from satisfactory.

3.3.3. Fouling Resistance Analysis

Flux represents membrane permeability and is inversely proportional to filtration resistance. The raw water was set as the control group, and the remaining second to eighth groups were added in the influent with 30 μM PMS, 30 μM Fe(III), 30 μM Fe(II)/30 μM PMS, 60 μM PMS, 60 μM Fe(III), 60 μM Fe(II)/60 μM PMS, and 120 μM Fe(II)/120 μM PMS. Figure 7a reveals the distribution law of the total filtration resistance, and Figure 7b shows the distribution law of the fouling layer resistance, which could further explain the flux changes in the previous section. The total resistance values of the eight groups were $4.49 \times 10^{11} \text{ m}^{-1}$, $4.34 \times 10^{11} \text{ m}^{-1}$, $3.16 \times 10^{11} \text{ m}^{-1}$, $2.99 \times 10^{11} \text{ m}^{-1}$, $3.46 \times 10^{11} \text{ m}^{-1}$, $2.98 \times 10^{11} \text{ m}^{-1}$, $2.77 \times 10^{11} \text{ m}^{-1}$, and $2.21 \times 10^{11} \text{ m}^{-1}$, respectively. Among them, the

fouling layer resistance accounted for a large proportion, the values of intrinsic membrane fouling resistance were approximately equal, and the membrane fouling caused by the raw water was the most serious. Under the condition of lower concentration, Fe(III) coagulation played a major role in reducing the total resistance (R_t) and intrinsic membrane fouling resistance (R_m), and PMS oxidation had limited effect on alleviating membrane fouling, because the altered effect of oxidation on functional groups was possible to increase the interaction of pollutants with the membrane. However, under the condition of higher concentration, as the concentration increased, PMS oxidation could further alleviate membrane fouling [55]. From the analysis of the reversibility of membrane fouling, according to the discussion of the previous section, after hydraulic backwashing, the initial membrane fluxes of the second and third cycles still had a large gap with the initial membrane fluxes of the operation. It can be seen that the recovery effect of membrane fluxes was limited, indicating that there was serious hydraulic irreversible fouling. As shown in Figure 7b, PMS oxidation could reduce the irreversible resistance (R_{ir}) and reversible resistance (R_r) to a certain extent, while Fe(III) coagulation could greatly reduce the irreversible resistance, which could be caused by larger size of the floc particles generated by coagulation, and some of the small substances that tend to block the membrane pores were absorbed at the same time. Under the condition of higher concentration, the dual effects of oxidation and coagulation produced by Fe(II)/PMS greatly reduced the proportion of irreversible resistance (R_{ir}) and increased the proportion of reversible resistance (R_r). This can be attributed to that Fe(II) was oxidized to Fe(III), which acted as a coagulant to adsorb small molecular substances that easily block the membrane pores, and at the same time, PMS was activated to generate $\bullet\text{OH}$ and $\text{SO}_4^{\bullet-}$, which oxidized and mineralized organic matter [22].

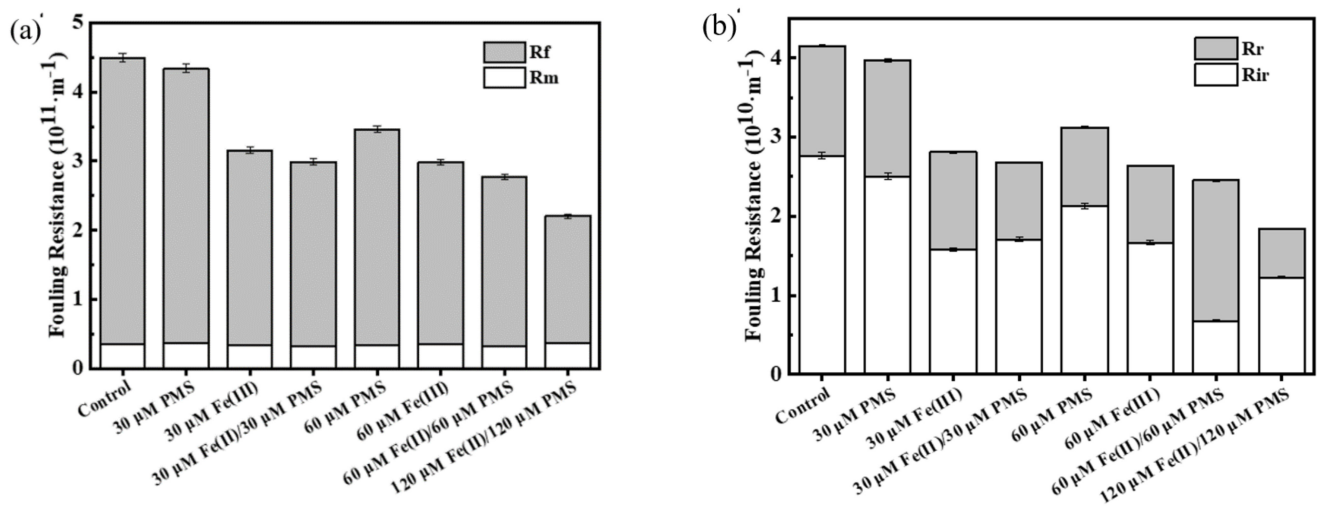


Figure 7. (a) Fouling resistance distributions of UF membrane (R_m) and fouling cake (R_f); (b) fouling resistance distributions of reversible (R_r) and irreversible (R_{ir}) fouling.

3.4. Oxidation Mechanism and Fouling Model Analysis

The fitting data of the fouling model for three periods of filtration are shown in Table S3. From the regression results, it can be seen that standard blocking and cake filtration were the main causes of membrane fouling, and no matter what the dosing conditions were, the fitting degree of each system was not much different, which may also be related to the dead-end filtering mode. Standard blocking is due to smaller particles adhering to the pores of the membrane, and cake filtration is due to the fact that the substances with larger particles are repelled by the narrow membrane pores, and they mutually adhere and deposit to form a filter cake layer, resulting in a decrease in flux [56]. Fe(II)/PMS created the best reversible and irreversible fouling mitigation performance. On the one hand, coagulation absorbed some small-molecule organic compounds, relieving the blockage of

membrane pores, and on the other hand, oxidation further removed organic matter on the basis of coagulation.

According to the reaction mechanism, it can be speculated that the removal of pollutants by Fe(II)/PMS is jointly mediated by $\bullet\text{OH}$ and $\text{SO}_4^{\bullet-}$, and the efficient degradation of fluorescent substances in raw water is promoted through the synergistic effect of oxidation and coagulation, which can be demonstrated by the EPR experiments. As shown in Figure 8, EPR spectra of different radicals captured by DMPO were simulated. No obvious peaks were observed in Fe(II) and PMS suspensions, indicating no free radical generation, while adduct characteristic signals of DMPO- SO_4 and DMPO-OH were observed in the Fe(II)/PMS suspension, indicating the formation of $\bullet\text{OH}$ and $\text{SO}_4^{\bullet-}$. $\text{SO}_4^{\bullet-}$ was generated by Fe(II)-activated PMS, and the peak intensity of DMPO- SO_4 was much lower than that of DMPO-OH, because the capture efficiency of $\bullet\text{OH}$ by DMPO was higher than that of $\text{SO}_4^{\bullet-}$ [57]. The mediated reaction mechanism is described as follows:

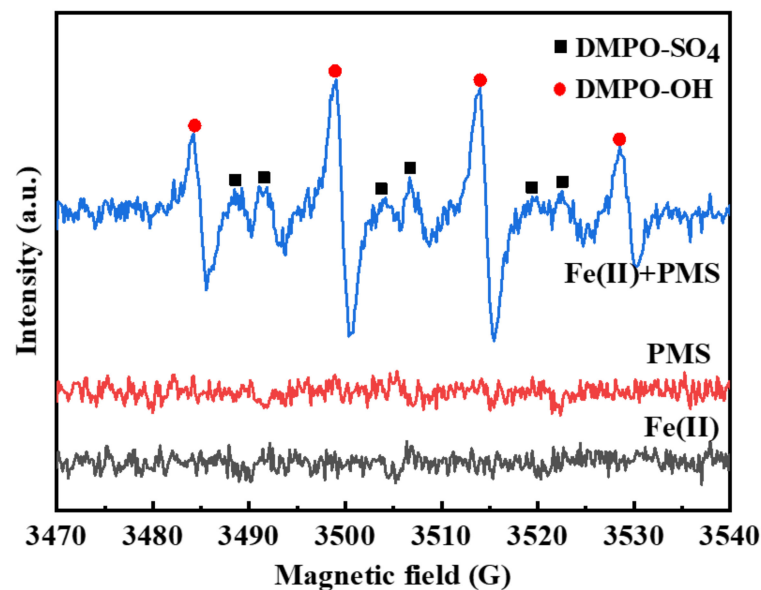
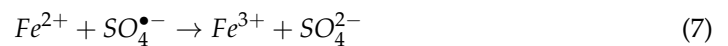
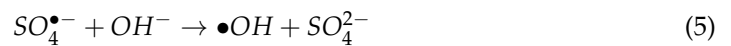
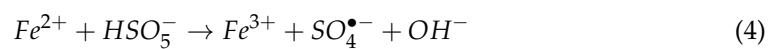


Figure 8. EPR spectra of Fe(II), PMS, and Fe(II)-activated PMS systems.

Sulfate radical ($\text{SO}_4^{\bullet-}$) and hydroxyl radical ($\bullet\text{OH}$) can be converted into each other, the reaction of Equation (5) occurs under alkaline conditions, and the reaction of Equation (6) occurs under acidic conditions. Fe(II) can react with $\bullet\text{OH}$ and $\text{SO}_4^{\bullet-}$, and be oxidized to Fe(III) to play the role of coagulant.

4. Conclusions

In this study, a novel method applying Fe(II)/PMS coupled UF for the treatment of secondary effluent from the Harbin Xinyi sewage treatment plant was proposed. The performance of Fe(III) coagulation, inactivated PMS pre-oxidation, and Fe(II)/PMS as pretreatment strategies for a UF system were evaluated separately. This research explored the optimal molar ratio in the experimental concentration range and the decontamination mechanism of Fe(II)/PMS, and the following conclusions were drawn:

- The Fe(II)-activated PMS coupled UF process can effectively reduce the content of pollutants in treating the secondary effluent of sewage treatment plants. The effect of removing organic matter, fluorescent components, and alleviating membrane fouling followed the order of Fe(II)/PMS > Fe(III) > inactivated PMS, and all three methods had good phosphorus removal effect, where coagulation played a major role in the removal of TP. The denitrification effect is less than satisfactory.
- Coagulation has a good removal effect on fluorescent components such as aromatic proteins and tryptophan-like components in organic matter, and the removal rate was proportional to the concentration of the coagulant.
- In terms of membrane fouling control, Fe(II)/PMS relied on the dual effects of coagulation and oxidation, and could produce synergistic effects at high concentrations (60 $\mu\text{mol/L}$), and the specific flux recovered from 0.19 LWH to 0.30 LWH, which was better than the two superimposed. This was because the combined use of Fe(II)/PMS at high concentrations can reduce the fouling of membrane pores and greatly reduce the proportion of irreversible resistance, so it can effectively alleviate membrane fouling.
- The pretreatment method has the advantages of low cost and less dosage of chemicals. When the concentration of Fe(II)/PMS was 60/60 $\mu\text{M}/\mu\text{M}$, i.e., the molar ratio was 1:1, membrane fouling was alleviated, and the specific flux (J/J_0) was improved. The total resistance, reversible resistance, and irreversible resistance were all the lowest, and the TP removal rate achieved over 99%. Fe(II) was oxidized into Fe(III), and at the same time, PMS was activated to generate $\text{SO}_4^{\bullet-}$ and $\bullet\text{OH}$, resulting in a synergistic effect of coagulation and oxidation, which was better than a single coagulation or oxidation process.

Supplementary Materials: The following supporting information can be downloaded at: <https://www.mdpi.com/article/10.3390/w14111726/s1>, Table S1: Characteristics of secondary effluent quality; Table S2: Fluorescence (EEM) intensity value of influent and effluent of UF process under different concentration conditions.; Table S3: Correlation coefficient (R^2) of membrane fouling models under different concentration conditions.

Author Contributions: Data curation, X.L. and S.Y.; Resources, A.D.; Writing—Original draft, X.L., R.C., Z.W. and W.L.; Writing—Review and Editing, W.L., R.Z. and A.D. All authors have read and agreed to the published version of the manuscript.

Funding: This research was jointly supported by National Natural Science Foundation of China (No. 52070058); State Key Laboratory of Urban Water Resource and Environment (Harbin Institute of Technology) (No. 2021TS17); the Natural Science Foundation of Heilongjiang Province (YQ2020E020); and the Heilongjiang Touyan Innovation Team Program (HIT-SE-01).

Institutional Review Board Statement: Not applicable for studies not involving human.

Informed Consent Statement: Not applicable for studies not involving human.

Acknowledgments: This research was jointly supported by National Natural Science Foundation of China (No. 52070058); State Key Laboratory of Urban Water Resource and Environment (Harbin Institute of Technology) (No. 2021TS17); the Natural Science Foundation of Heilongjiang Province (YQ2020E020); and the Heilongjiang Touyan Innovation Team Program (HIT-SE-01).

Conflicts of Interest: The authors declare no conflict of interest.

References

1. Lv, H.; Yang, L.; Zhou, J.; Zhang, X.; Wu, W.; Li, Y.; Jiang, D. Water resource synergy management in response to climate change in China: From the perspective of urban metabolism. *Resour. Conserv. Recycl.* **2020**, *163*, 105095. [[CrossRef](#)]
2. Turning “Used Water” into Resources. Available online: <https://iwa-network.org/turning-used-water-into-resources/> (accessed on 26 February 2015).
3. Zhou, Q.; Sun, H.; Jia, L.; Wu, W.; Wang, J. Simultaneous biological removal of nitrogen and phosphorus from secondary effluent of wastewater treatment plants by advanced treatment: A review. *Chemosphere* **2022**, *296*, 134054. [[CrossRef](#)]
4. Hu, Y.; Cheng, H. Water pollution during China’s industrial transition. *Environ. Dev.* **2013**, *8*, 57–73. [[CrossRef](#)]

5. Paraskeva, P.; Graham, N.J.D. Treatment of a secondary municipal effluent by ozone, UV and microfiltration: Microbial reduction and effect on effluent quality. *Desalination* **2005**, *186*, 47–56. [[CrossRef](#)]
6. Acero, J.L.; Benitez, F.J.; Leal, A.I.; Real, F.J.; Teva, F. Membrane filtration technologies applied to municipal secondary effluents for potential reuse. *J. Hazard. Mater.* **2010**, *177*, 390–398. [[CrossRef](#)]
7. Liu, X.; Ren, Z.; Ngo, H.H.; He, X.; Desmond, P.; Ding, A. Membrane technology for rainwater treatment and reuse: A mini review. *Water Cycle* **2021**, *2*, 51–63. [[CrossRef](#)]
8. Gao, W.; Liang, H.; Ma, J.; Han, M.; Chen, Z.-L.; Han, Z.-S.; Li, G.-B. Membrane fouling control in ultrafiltration technology for drinking water production: A review. *Desalination* **2011**, *272*, 1–8. [[CrossRef](#)]
9. Shi, X.; Tal, G.; Hankins, N.P.; Gitis, V. Fouling and cleaning of ultrafiltration membranes: A review. *J. Water Process Eng.* **2014**, *1*, 121–138. [[CrossRef](#)]
10. Henderson, R.; Subhi, N.; Antony, A.; Khan, S.J.; Murphy, K.; Leslie, G.L.; Chen, V.; Stuetz, R.M.; Le-Clech, P. Evaluation of effluent organic matter fouling in ultrafiltration treatment using advanced organic characterisation techniques. *J. Membr. Sci.* **2011**, *382*, 50–59. [[CrossRef](#)]
11. Tian, J.-Y.; Ernst, M.; Cui, F.; Jekel, M. Correlations of relevant membrane foulants with UF membrane fouling in different waters. *Water Res.* **2013**, *47*, 1218–1228. [[CrossRef](#)]
12. Peiris, R.; Jaklewicz, M.; Budman, H.; Legge, R.; Moresoli, C. Assessing the role of feed water constituents in irreversible membrane fouling of pilot-scale ultrafiltration drinking water treatment systems. *Water Res.* **2013**, *47*, 3364–3374. [[CrossRef](#)] [[PubMed](#)]
13. Wang, H.; Qu, F.; Ding, A.; Liang, H.; Jia, R.; Li, K.; Bai, L.; Chang, H.; Li, G. Combined effects of PAC adsorption and in situ chlorination on membrane fouling in a pilot-scale coagulation and ultrafiltration process. *Chem. Eng. J.* **2016**, *283*, 1374–1383. [[CrossRef](#)]
14. Yu, W.; Graham, N.J.D. Application of Fe(II)/K₂MnO₄ as a pre-treatment for controlling UF membrane fouling in drinking water treatment. *J. Membr. Sci.* **2015**, *473*, 283–291. [[CrossRef](#)]
15. Bai, L.; Liu, Z.; Wang, H.; Li, G.; Liang, H. Fe(II)-activated peroxymonosulfate coupled with nanofiltration removes natural organic matter and sulfamethoxazole in natural surface water: Performance and mechanisms. *Sep. Purif. Technol.* **2021**, *274*, 119088. [[CrossRef](#)]
16. Yu, W.; Graham, N.J.; Fowler, G.D. Coagulation and oxidation for controlling ultrafiltration membrane fouling in drinking water treatment: Application of ozone at low dose in submerged membrane tank. *Water Res.* **2016**, *95*, 1–10. [[CrossRef](#)]
17. Rastogi, A.; Al-Abed, S.R.; Dionysiou, D.D. Sulfate radical-based ferrous–peroxymonosulfate oxidative system for PCBs degradation in aqueous and sediment systems. *Appl. Catal. B Environ.* **2009**, *85*, 171–179. [[CrossRef](#)]
18. Zou, J.; Ma, J.; Chen, L.; Li, X.; Guan, Y.; Xie, P.; Pan, C. Rapid Acceleration of Ferrous Iron/Peroxymonosulfate Oxidation of Organic Pollutants by Promoting Fe(III)/Fe(II) Cycle with Hydroxylamine. *Environ. Sci. Technol.* **2013**, *47*, 11685–11691. [[CrossRef](#)]
19. Cheng, X.; Liang, H.; Ding, A.; Tang, X.; Liu, B.; Zhu, X.; Gan, Z.; Wu, D.; Li, G. Ferrous iron/peroxymonosulfate oxidation as a pretreatment for ceramic ultrafiltration membrane: Control of natural organic matter fouling and degradation of atrazine. *Water Res.* **2017**, *113*, 32–41. [[CrossRef](#)]
20. Yang, M.; Hasaer, B.; Bai, Y.; Liu, R.; Hu, C.; Qu, J. Using activated peroxymonosulfate by electrochemically generated FeII for conditioning and dewatering of anaerobically digested sludge. *Chem. Eng. J.* **2019**, *391*, 123603. [[CrossRef](#)]
21. Ling, L.; Zhang, D.; Fan, C.; Shang, C. A Fe(II)/citrate/UV/PMS process for carbamazepine degradation at a very low Fe(II)/PMS ratio and neutral pH: The mechanisms. *Water Res.* **2017**, *124*, 446–453. [[CrossRef](#)]
22. Cheng, X.; Liang, H.; Ding, A.; Zhu, X.; Tang, X.; Gan, Z.; Xing, J.; Wu, D.; Li, G. Application of Fe(II)/peroxymonosulfate for improving ultrafiltration membrane performance in surface water treatment: Comparison with coagulation and ozonation. *Water Res.* **2017**, *124*, 298–307. [[CrossRef](#)] [[PubMed](#)]
23. Nielsen, S.S. *Phenol-Sulfuric Acid Method for Total Carbohydrates*; Springer: New York, NY, USA, 2010.
24. Schuler, M.A.; Zielinski, R.E. *3B-Lowry Assay for Protein Determination*; Academic Press: Cambridge, MA, USA, 1989.
25. Derradji, A.; Taha, S.; Dorange, G. Application of the resistances in series model in ultrafiltration. *Desalination* **2005**, *184*, 377–384. [[CrossRef](#)]
26. Lin, C.-F.; Lin, A.; Chandana, P.S.; Tsai, C.-Y. Effects of mass retention of dissolved organic matter and membrane pore size on membrane fouling and flux decline. *Water Res.* **2009**, *43*, 389–394. [[CrossRef](#)] [[PubMed](#)]
27. Bowen, W.R.; Calvo, J.I.; Hernandez, A. Steps of membrane blocking in flux decline during protein microfiltration. *J. Membr. Sci.* **1995**, *101*, 153–165. [[CrossRef](#)]
28. Shen, Y.; Zhao, W.; Xiao, K.; Huang, X. A systematic insight into fouling propensity of soluble microbial products in membrane bioreactors based on hydrophobic interaction and size exclusion. *J. Membr. Sci.* **2010**, *346*, 187–193. [[CrossRef](#)]
29. Duan, J.; Gregory, J. Coagulation by hydrolysing metal salts. *Adv. Colloid Interface Sci.* **2003**, *100–102*, 475–502. [[CrossRef](#)]
30. Sillanpää, M.; Ncibi, M.C.; Matilainen, A.; Vepsäläinen, M. Removal of natural organic matter in drinking water treatment by coagulation: A comprehensive review. *Chemosphere* **2018**, *190*, 54–71. [[CrossRef](#)]

31. Matilainen, A.; Vepsäläinen, M.; Sillanpää, M. Natural organic matter removal by coagulation during drinking water treatment: A review. *Adv. Colloid Interface Sci.* **2010**, *159*, 189–197. [[CrossRef](#)]
32. Liu, J.; Peng, C.; Shi, X. Preparation, characterization, and applications of Fe-based catalysts in advanced oxidation processes for organics removal: A review. *Environ. Pollut.* **2021**, *293*, 118565. [[CrossRef](#)]
33. Zhang, X.; Ma, Y.; Tang, T.; Xiong, Y.; Dai, R. Removal of cyanobacteria and control of algal organic matter by simultaneous oxidation and coagulation-comparing the H₂O₂/Fe(II) and H₂O₂/Fe(III) processes. *Sci. Total Environ.* **2020**, *720*, 137653. [[CrossRef](#)]
34. Leenheer, J.A.; Croué, J.-P. Peer Reviewed: Characterizing Aquatic Dissolved Organic Matter. *Environ. Sci. Technol.* **2003**, *37*, 18A–26A. [[CrossRef](#)] [[PubMed](#)]
35. Peng, Y.; Tang, H.; Yao, B.; Gao, X.; Yang, X.; Zhou, Y. Activation of peroxymonosulfate (PMS) by spinel ferrite and their composites in degradation of organic pollutants: A Review. *Chem. Eng. J.* **2021**, *414*, 128800. [[CrossRef](#)]
36. Reddy, D.H.K.; Yun, Y.-S. Spinel ferrite magnetic adsorbents: Alternative future materials for water purification? *Coord. Chem. Rev.* **2016**, *315*, 90–111. [[CrossRef](#)]
37. Metzger, U.; Le-Clech, P.; Stuetz, R.M.; Frimmel, F.H.; Chen, V. Characterisation of polymeric fouling in membrane bioreactors and the effect of different filtration modes. *J. Membr. Sci.* **2007**, *301*, 180–189. [[CrossRef](#)]
38. Zhang, C.; Bao, Q.; Wu, H.; Shao, M.; Wang, X.; Xu, Q. Impact of polysaccharide and protein interactions on membrane fouling: Particle deposition and layer formation. *Chemosphere* **2022**, *296*, 134056. [[CrossRef](#)]
39. Neemann, F.; Rosenberger, S.; Jefferson, B.; McAdam, E.J. Non-covalent protein–polysaccharide interactions and their influence on membrane fouling. *J. Membr. Sci.* **2013**, *446*, 310–317. [[CrossRef](#)]
40. Ushani, U.; Lu, X.; Wang, J.; Zhang, Z.; Dai, J.; Tan, Y.; Wang, S.; Li, W.; Niu, C.; Cai, T.; et al. Sulfate radicals-based advanced oxidation technology in various environmental remediation: A state-of-the-art review. *Chem. Eng. J.* **2020**, *402*, 126232. [[CrossRef](#)]
41. Matilainen, A.; Gjessing, E.T.; Lahtinen, T.; Hed, L.; Bhatnagar, A.; Sillanpää, M. An overview of the methods used in the characterisation of natural organic matter (NOM) in relation to drinking water treatment. *Chemosphere* **2011**, *83*, 1431–1442. [[CrossRef](#)]
42. Cheng, W.P.; Chi, F.H. A study of coagulation mechanisms of polyferric sulfate reacting with humic acid using a fluorescence-quenching method. *Water Res.* **2002**, *36*, 4583–4591. [[CrossRef](#)]
43. Yu, H.; Qu, F.; Wu, Z.; He, J.; Rong, H.; Liang, H. Front-face fluorescence excitation-emission matrix (FF-EEM) for direct analysis of flocculated suspension without sample preparation in coagulation-ultrafiltration for wastewater reclamation. *Water Res.* **2020**, *187*, 116452. [[CrossRef](#)]
44. Zhang, W.; Jin, X.; Liu, D.; Lang, C.; Shan, B. Temporal and spatial variation of nitrogen and phosphorus and eutrophication assessment for a typical arid river—Fuyang River in northern China. *J. Environ. Sci.* **2017**, *55*, 41–48. [[CrossRef](#)] [[PubMed](#)]
45. Ying, F.; Jichao, Z.; Yanzheng, W.; Yanzhen, Y. Resource preparation of poly-Al-Zn-Fe (PAZF) coagulant from galvanized aluminum slag: Characteristics, simultaneous removal efficiency and mechanism of nitrogen and organic matters. *Chem. Eng. J.* **2012**, *203*, 301–308. [[CrossRef](#)]
46. Liu, T.; Lian, Y.; Graham, N.; Yu, W.; Rooney, D.; Sun, K. Application of polyacrylamide flocculation with and without alum coagulation for mitigating ultrafiltration membrane fouling: Role of floc structure and bacterial activity. *Chem. Eng. J.* **2016**, *307*, 41–48. [[CrossRef](#)]
47. Bai, S.; Zhu, Y.; Zhang, X.; Zhang, H.; Gong, Y. Enhanced Phosphorus Removal from Municipal Wastewater by Coagulation with Alum and Iron Salts. In Proceedings of the International Conference on Bioinformatics and Biomedical Engineering, ICBBE 2010, Chengdu, China, 18–20 June 2010; pp. 1–4. [[CrossRef](#)]
48. Fytianos, K.; Voudrias, E.; Raikos, N. Modelling of phosphorus removal from aqueous and wastewater samples using ferric iron. *Environ. Pollut.* **1998**, *101*, 123–130. [[CrossRef](#)]
49. GB 3838-2002; Environmental quality standards for surface water. State Environmental Protection Administration: Beijing, China, 2002.
50. Zhang, B.; Mao, X.; Tang, X.; Tang, H.; Shen, Y.; Shi, W. Pre-coagulation for membrane fouling mitigation in an aerobic granular sludge membrane bioreactor: A comparative study of modified microbial and organic flocculants. *J. Membr. Sci.* **2021**, *644*, 120129. [[CrossRef](#)]
51. Fan, J.; Lin, T.; Chen, W.; Xu, H.; Tao, H. Control of ultrafiltration membrane fouling during the recycling of sludge water based on Fe(II)-activated peroxymonosulfate pretreatment. *Chemosphere* **2020**, *246*, 125840. [[CrossRef](#)]
52. Dayarathne, H.; Angove, M.J.; Aryal, R.; Abuel-Naga, H.; Mainali, B. Removal of natural organic matter from source water: Review on coagulants, dual coagulation, alternative coagulants, and mechanisms. *J. Water Process Eng.* **2020**, *40*, 101820. [[CrossRef](#)]
53. Ding, Y.; Wang, X.; Fu, L.; Peng, X.; Pan, C.; Mao, Q.; Wang, C.; Yan, J. Nonradicals induced degradation of organic pollutants by peroxydisulfate (PDS) and peroxymonosulfate (PMS): Recent advances and perspective. *Sci. Total Environ.* **2020**, *765*, 142794. [[CrossRef](#)]
54. Lee, J.; Von Gunten, U.; Kim, J.-H. Persulfate-Based Advanced Oxidation: Critical Assessment of Opportunities and Roadblocks. *Environ. Sci. Technol.* **2020**, *54*, 3064–3081. [[CrossRef](#)]

55. Li, K.; Wen, G.; Li, S.; Chang, H.; Shao, S.; Huang, T.; Li, G.; Liang, H. Effect of pre-oxidation on low pressure membrane (LPM) for water and wastewater treatment: A review. *Chemosphere* **2019**, *231*, 287–300. [[CrossRef](#)]
56. Qu, F.; Liang, H.; Zhou, J.; Nan, J.; Shao, S.; Zhang, J.; Li, G. Ultrafiltration membrane fouling caused by extracellular organic matter (EOM) from *Microcystis aeruginosa*: Effects of membrane pore size and surface hydrophobicity. *J. Membr. Sci.* **2013**, *449*, 58–66. [[CrossRef](#)]
57. Qin, W.; Fang, G.; Wang, Y.; Zhou, D. Mechanistic understanding of polychlorinated biphenyls degradation by peroxydisulfate activated with CuFe₂O₄ nanoparticles: Key role of superoxide radicals. *Chem. Eng. J.* **2018**, *348*, 526–534. [[CrossRef](#)]